



Contents lists available at ScienceDirect

Spectrochimica Acta Part A: Molecular and Biomolecular Spectroscopy

journal homepage: www.elsevier.com/locate/saa

Conformational state of β -hydroxynaphthylamides: Barriers for the rotation of the amide group around CN bond and dynamics of the morpholine ring



Tomasz Kozlecki^a, Peter M. Tolstoy^{b,*}, Agnieszka Kwocz^c, Mikhail A. Vovk^b, Andrzej Kochel^c, Izabela Polowczyk^a, Peter Yu. Tretyakov^d, Aleksander Filarowski^{c,e,*}

^aWrocław University of Technology, Faculty of Chemistry, Division of Chemical Engineering, 50-373 Wrocław, Poland

^bSt. Petersburg State University, Center for Magnetic Resonance, 198504 St. Petersburg, Russia

^cFaculty of Chemistry, University of Wrocław, 50-383 Wrocław, Poland

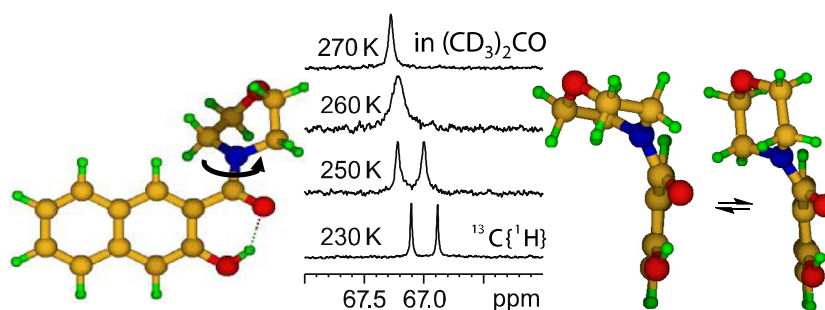
^dUniversity of Architecture and Civil Engineering, 625001 Tyumen, Russia

^eThe Joint Institute for Nuclear Research, Frank Laboratory of Neutron Physics, 141980 Dubna, Russia

HIGHLIGHTS

- Morpholine, pyrrolidine and dimethylamine derivatives of *ortho*-hydroxynaphthalene (non-planar, OHO bonded).
- Dynamic NMR study: CN rotation barriers 13–19 kcal/mol.
- Intramolecular OHO bond strength influences CN rotation barrier height.
- Morpholine chair–chair ‘ring flips’ (ca. 5 kcal/mol barrier) evidence by ¹H NMR and DFT.

GRAPHICAL ABSTRACT



ARTICLE INFO

Article history:

Received 18 March 2015

Received in revised form 14 April 2015

Accepted 16 April 2015

Available online 28 April 2015

Keywords:

β -Hydroxynaphthylamides

Amide group rotation

Intramolecular hydrogen bond

Conformational isomerism

Solvent effects

DNMR

ABSTRACT

Three β -hydroxynaphthylamides (morpholine, pyrrolidine and dimethylamine derivatives) have been synthesized and their conformational state was analyzed by NMR, X-ray and DFT calculations. In aprotic solution the molecules contain intramolecular OHO hydrogen bonds, which change into intermolecular ones in solid state. The energy barriers for the amide group rotation around the CN bond were estimated from the line shape analysis of ¹H and ¹³C NMR signals. A tentative correlation between the barrier height and the strength of OHO bond was proposed. Calculations of the potential energy profiles for the rotations around CC and CN bonds were done. In case of morpholine derivative experimental indications of additional dynamics: chair–chair ‘ring flip’ in combination with the twisting around CC bond were obtained and confirmed by quantum chemistry calculations.

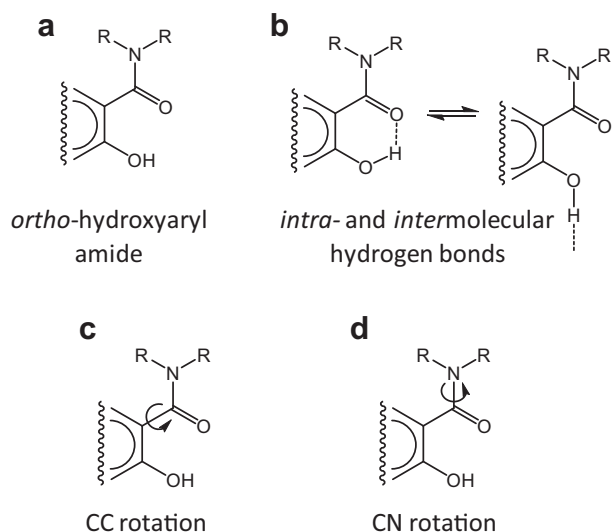
© 2015 Elsevier B.V. All rights reserved.

* Corresponding authors at: Faculty of Chemistry, University of Wrocław, 50-383 Wrocław, Poland (A. Filarowski).

E-mail addresses: peter.tolstoy@spbu.ru (P.M. Tolstoy), aleksander.filarowski@chem.uni.wroc.pl (A. Filarowski).

Introduction

Conformational research of amide group has been of constant scientific interest for many years because this type of formation composes fragments of the peptide bond in proteins [1–4]. Conformational research of aryl amides has also attracted

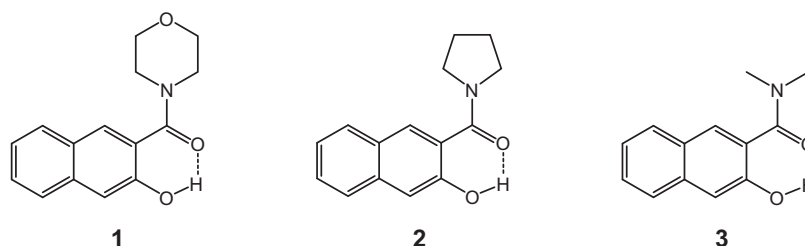


Scheme 1. General structure of *ortho*-hydroxyaryl amides (a) and some of the possible dynamic processes: an equilibrium between *intra*- and *intermolecular* hydrogen bonds (b) and rotation of the amide group around CC bond (c) or CN bond (d).

significant attention and such compounds can even be considered one of the classical examples for study of conformational equilibrium [5–10] *ortho*-hydroxyaryl amides ('a' in Scheme 1) add to this some complexity due to the ability of the OH group to form various hydrogen bonds [11–14]. Such compounds are subject to several dynamic processes: an equilibrium between *intra*- and *intermolecular* hydrogen bonds ('b' in Scheme 1), and – similar to other amides – rotation of the amide group around CC and CN bonds ('c' and 'd' in Scheme 1) [15–20].

Note that *ortho*-hydroxyaryl amides do not exhibit intramolecular proton transfer despite the strong acid–base interaction between the hydroxyl group and the carbonyl group of the amide [15]. A different situation is observed for *ortho*-hydroxyaryl Schiff [21,22], Mannich bases [23,24] and *ortho*-hydroxy arylaza derivatives [25–27] where the geometry of the intramolecular H-bond depends to a great extent on the electron-donating and electron-accepting properties of the substituents on the nitrogen atom and on the phenolic moiety [28] However, these conformational transformations are not characteristic for salicylamides. It has been proposed that the most significant factor contributing to the conformational state of salicylamides is the steric interaction between phenolic moiety and bulky substituents of the amide group [15]. It is also needed to be pointed out that the basicity of the amide nitrogen is generally too low for the intramolecular OHN hydrogen bond to form with the OH proton (after a 180° rotation around the CC bond).

In this paper we present the synthesis and studies of three *ortho*-hydroxynaphthalene amides by means of variable-temperature NMR spectroscopy, X-ray diffraction and quantum-mechanical calculations. The main goal is to study conformation and dynamics of the (3-hydroxynaphthalen-2-yl)(morpholin-4-yl)methanone **1**, (3-hydroxynaphthalen-2-yl)(pyrrolidin-1-yl)methanone **2** and



Scheme 2. Structures of *ortho*-hydroxynaphthyl amides studied in this work (the hydrogen bonded state and the non-planarity of the structures is discussed in the text).

3-hydroxy-*N,N*-dimethylnaphthalene-2-carboxamide **3** (Scheme 2) dissolved in various organic solvents. The experimental and theoretical approaches used in this work are well-established and applied here as a tool to study the new set of compounds.

Materials and methods

Synthesis

The studied compounds were synthesized under microwave irradiation from methyl 3-hydroxy-2-naphthoate and an excess of appropriate amine. The reactions were carried out using a CEM Discover Synthesis Unit (CEM Corp., Matthews, NC) and performed in 10 mL glass vessels sealed with a septum. The pressure was controlled by a load cell connected to the vessel for an indirect measurement. The temperature was monitored using a calibrated infrared temperature control. The synthesis was carried out using the magnetic stirring. Reaction progress was monitored using chemical ionization mass spectrometry on a HP 5989A MS Engine, with methane as a reagent gas.

For the synthesis of **1** a mixture of methyl 3-hydroxy-2-naphthoate (501 mg, 2.48 mmol) and morpholine (1.5 mL) was placed in the pressure vial and irradiated for 5 min at 175 °C/275 psi with maximum microwave power set at 100 W. Reaction mixture was cooled down, dissolved in chloroform (75 mL) and extracted first with aqueous hydrochloric acid (3 × 75 mL) and then with water (2 × 75 mL). Organic phase was dried over magnesium sulfate and filtered, then the solvent was evaporated and the remaining substance was purified by column chromatography (silica gel 60, 70–230 mesh; eluent: ethyl acetate). As some impurities were detected by TLC, chromatography was repeated (silica gel 60, 70–230 mesh; eluent: ethyl acetate–heptane, 1:1). Purified product was recrystallized from methanol.

Synthesis of **2** was carried out as described above, using methyl 3-hydroxy-2-naphthoate (499 mg, 2.47 mmol) and pyrrolidine (1.5 mL). A single chromatographic column (silica gel 60, 70–230 mesh; eluent: ethyl acetate) was sufficient to purify the product, which was then recrystallized from methanol.

Synthesis of **3** was carried out in a similar fashion. A mixture of methyl 3-hydroxy-2-naphthoate (499 mg, 2.47 mmol), dioxane (2 mL) and 40% aqueous diethylamine (1.5 mL) was irradiated. The purification was carried out as described above, single chromatographic purification (silica gel 60, 70–230 mesh; eluent: ethyl acetate) was sufficient, after which the product was recrystallized from methanol.

DFT calculations

Quantum mechanical calculations were carried out using GAUSSIAN09 program [29] at the DFT (B3LYP) level of theory [30,31] with the 6-31+G(d,p) basis set [32], suitable for the H-bonded systems [33] potential energy profiles were calculated by changing and fixing the corresponding angles in 10-degree steps, and optimizing all other geometric parameters.

X-ray diffraction studies of **1** and **3**

The intensity data were collected at 100 K using a X-Calibur Ruby diffractometer and graphite-monochromated MoK α (0.71073 Å) radiation generated from an X-ray tube operating at 50 kV and 35 mA. The images were indexed, integrated, and scaled using the Oxford Diffraction data reduction package [34]. The experimental details together with crystallographic data for both compounds are given in Supplementary data (Table S1). A multi-scan absorption correction was applied. The structure was solved by direct methods using SHELXS97 [35] and refined by the full-matrix least-squares method on all F^2 data (SHELXL97) [36]. Non-hydrogen atoms were refined with anisotropic thermal parameters; hydrogen atoms were included from $\Delta\rho$ maps and refined isotropically. The Supplementary crystallographic data for this paper are under CCDC No. 960172 for (3-hydroxynaphthalen-2-yl)(morpholin-4-yl)methanone (**1**) and CCDC No. 960171 for 3-hydroxy-*N,N*-dimethylnaphthalene-2-carboxamide (**3**). These data can be obtained free of charge via www.ccdc.cam.ac.uk/conts/retrieving.html (or from the Cambridge Crystallographic Data Centre, 12 Union Road, Cambridge CB2 1EZ, UK; fax: (+44) 1123-336-033, e-mail: deposit@ccdc.cam.ac.uk).

NMR measurements

Samples for NMR measurements were prepared by placing 8 mg of substance (4 mg in case of poorly soluble compounds) in a standard 5 mm NMR sample tube and adding 0.7 mL of a solvent using Eppendorf pipette. Deuterated solvents CDCl₃, (CD₃)₂CO, CD₃OD

and tetrahydrofuran-*d*₈ were purchased from Prikladnaja Khimija (Russia) and used without further purification. NMR measurements were performed at the Center for Magnetic Resonance, St. Petersburg State University. The ¹H and ¹³C{¹H} NMR spectra were recorded on a Bruker Avance III 500 MHz spectrometer (500.03 MHz for ¹H, 125.73 MHz for ¹³C). The spectra were measured using the solvent peak as internal reference, and the chemical shifts were converted to the conventional TMS scale. The pulse delay for 30° pulses was 1–2 s for ¹H and 2 s for ¹³C{¹H} power-gated NMR spectra. The number of scans varied between 128–256 for ¹H and 1024–4096 for ¹³C{¹H} NMR spectra. Sample temperature was stabilized with the precision of ± 1 °C. Spectra were processed using Topspin 3.2 Software and line shape analysis was performed using the built-in program DNMR and Origin 9.0.

Results and discussion

NMR spectroscopy is often a method of choice to study H-bonding, specific molecular conformations and hindered internal rotations in solution [37–40]. For example, variable-temperature ¹H, ¹³C and ¹⁵N NMR has been previously successfully used to study hydrogen bond geometries in polar aprotic environment [41,42], inter- and intramolecular proton tautomerism [25,43], conformational isomerism [44,45] and other phenomena. In this work we also start our discussion with the temperature-dependent ¹H and ¹³C NMR spectra of compounds **1**, **2** and **3** dissolved in CDCl₃, (CD₃)₂CO, CD₃OD or tetrahydrofuran-*d*₈ (THF-*d*₈), presented in Fig. 1 and in Figs. S1–S5 of Supplementary data. Here we describe in details the spectra

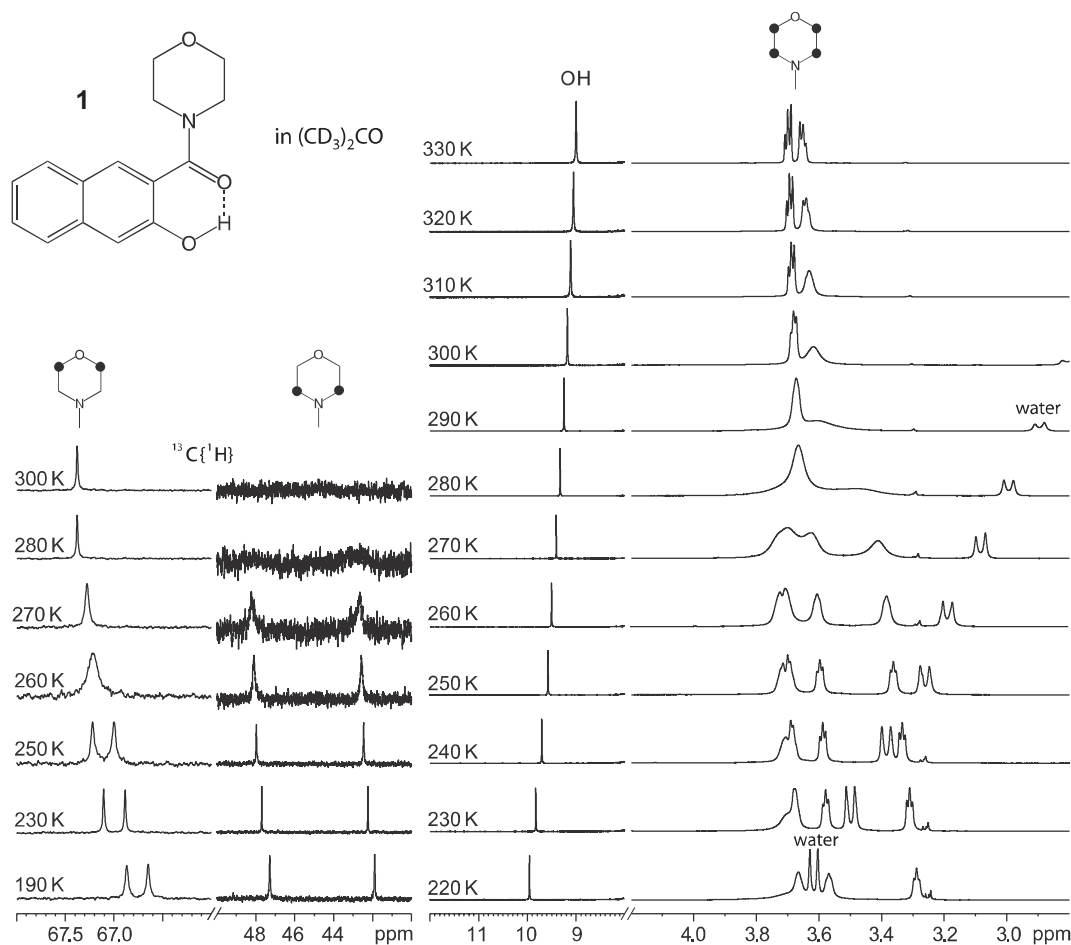


Fig. 1. Parts of variable-temperature ¹H and ¹³C{¹H} NMR spectra of **1** dissolved in (CD₃)₂CO. Assignment of signals to particular nuclei of alkyl group is given by black circles.

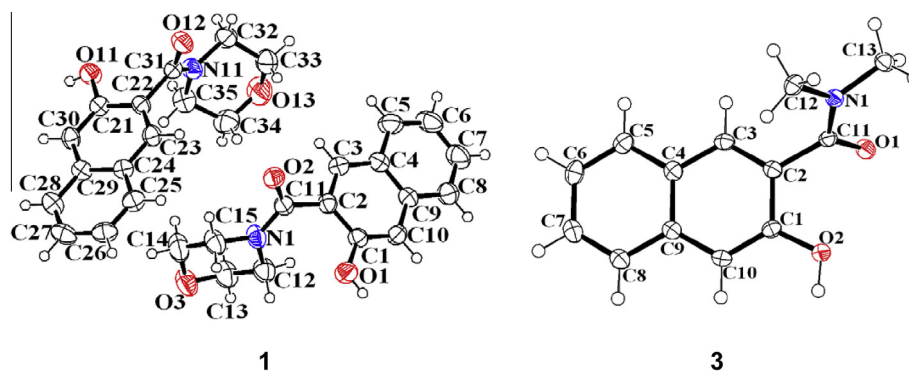


Fig. 2. The molecular structures and atom labeling scheme of **1** and **3** obtained by X-ray diffraction.

of **1** dissolved in $(\text{CD}_3)_2\text{CO}$, while other spectra can be analyzed in a similar way. Note that due to the low solubility not all combinations of compounds and solvents have been studied in this work.

The chemical shift of the OH proton signal of **1** of about 10 ppm indicates that this group is involved in a medium-strong hydrogen bond. Judging from the similar values of OH chemical shifts of **1** in other solvents (9–11 ppm, see Figs. S1 and S2), absence of concentration-dependence of OH chemical shifts, quantum mechanical calculations (see below) and steric considerations, the hydrogen bond is intramolecular OH \cdots O bond. The OH signal shifts from 9 ppm at 330 K to 10 ppm at 220 K, which reflects H-bond strengthening upon cooling [46]. Most probably, this is because in the molecule with stronger (shorter) H-bond due to the electron transfer the local polarity of the OHO bridge is larger (indeed, the hypothetical limiting structure is $\text{O}^+\text{H}\cdots\text{O}^-$) [40,47], which leads to the preferential stabilization of such structures at lower temperatures, when solvent polarity (dielectric constant) increases [48]. For **1** dissolved in other solvents, as well as for **2** and **3** in various solvents, the sensitivity of the OH chemical shifts to temperature is comparable. There are no spectral indications of the amide group rotation around the CC bond, which would lead to the breakage of OH \cdots O bond and possible formation of an intramolecular OH \cdots N bond, which is unlikely due the low basicity of the nitrogen atom. Besides, there is no interaction of OH protons of **1** with OH protons of residual water: in the whole temperature range the H_2O and HDO signals are resolved, relatively sharp and shift to 3.6 ppm upon cooling. To summarize, we arrive to the conformation of **1** as shown in Scheme 2, with an intramolecular OHO hydrogen bond. For **2** and **3** the reasoning is similar. It should be pointed out that the presence of OHO hydrogen bonds does not mean that the molecules are planar. In fact, there is enough evidence of their non-planarity (see below). The intramolecular OHO bonds for **1** and **3** are broken in crystalline state (see Fig. 2; visualized using the program Mercury CSD version 2.2) [49], where these molecules form infinite H-bonded chains. Crystallographic parameters for these intermolecular hydrogen bonds are collected in Table 1. In other words, the H-bonding and conformational state of molecules such as **1–3** is dependent of their immediate surroundings and both experimental and computational efforts are valuable in tackling this issue.

The ^1H and ^{13}C NMR spectra clearly show that protons and carbon atoms of the morpholine group of **1** are involved in a hindered rotation around CN bond. This dynamic process is fast in NMR time scale at room temperature and gradually slows down when the temperature is lowered. At 250 K signals of OCH_2 and NCH_2 carbon atoms of the morpholine group split into pairs; at the same time, four proton signals become visible in the ^1H NMR spectrum. Line shape analysis of the OCH_2 carbon signals resulted in the estimated

Table 1

X-ray crystallographic hydrogen bond parameters for **1** and **3** [Å and degrees].

Compound	Type of H-bond	$r(\text{O}\cdots\text{H})$	$r(\text{H}\cdots\text{O})$	$r(\text{O}\cdots\text{O})$	$\Theta(\text{OHN})$
1	$\text{O}(1)\text{--H}(10)\cdots\text{O}(2)$	0.82	1.86	2.673(2)	175
	$\text{O}(11)\text{--H}(110)\cdots\text{O}(12)$	0.82	1.88	2.693(2)	169
3	$\text{O}(2)\text{--H}(10)\cdots\text{O}(1)$	0.94	1.73	2.638(1)	163

rates of the hindered rotation at each temperature. Arrhenius plot of these rates is presented in Fig. 3.

Estimated barrier height is about $E_a = 15.4 \pm 0.6$ kcal/mol. Note, that the estimation of the barrier height requires extrapolation of the temperature dependence of intrinsic chemical shifts to higher temperatures, the procedure which is illustrated in Fig. S6 of the Supplementary data. Similar process of line shape analysis and Arrhenius plot fitting was repeated for ^1H and ^{13}C NMR spectra of **1**, **2** and **3** dissolved in other solvents (the chemical shift extrapolation was polynomial and minimal power of the polynomial was chosen every time, usually a straight line or a parabola). In some solvents at low temperatures the signals of CH_2 protons of **1** and **2** are split into multiplets due to spin–spin couplings and further on due to the chemical non-equivalence induced by the non-planarity of the molecule (see below). As was mentioned above, at intermediate temperatures there is no indication of rotation around C–C bond: OHO hydrogen bond appears to be intact over the whole temperature range and even if there would be a rotation around CC bond we do not expect to see its effect on the signals of CH_2 protons (a full 360° rotation would not interchange them and a 180° rotation requires an OHN hydrogen bond, which is unlikely). However, the line broadening at lowest temperatures might be associated with some dynamics involving rotation around the CC bond, a topic to which we will return below.

Plots of fitted chemical shifts as well as rate constants of CN rotation can be found in Figs. S7–S19 of Supplementary data. The results on the amide group rotational barrier heights are collected in Table 2. The trend obtained for E_a correlates pretty well with the data obtained previously for salicylamide, see Ref. [15] (some difference might be explained by an arguably less accurate method in the determination of E_a used in Ref. [15]). There are at least three effects which can influence the barrier height for the rotation around the CN bond. Firstly, the more bulky substituents on the amide nitrogen atom might sterically hinder the rotation due to the interaction with the aromatic proton on the naphthalene group. Secondly, the partial electron transfer to the carbonyl oxygen atom due to the formation of the intramolecular OH \cdots O hydrogen bond would increase the double-bond character of the CN bond and further slow down the amide rotation. Finally, the non-specific interaction with the solvent might influence the barrier height. Though the body of data presented in this work is

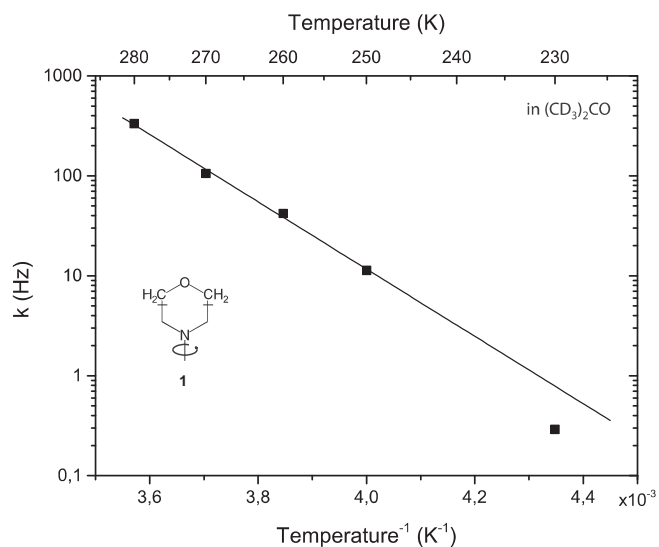


Fig. 3. Arrhenius plot of the rate constants of the amide group rotation around CN bond of **1** dissolved in $(\text{CD}_3)_2\text{CO}$, obtained by line shape analysis of ^{13}C NMR spectra. Solid line represents a least square linear fit.

Table 2

Energy barriers E_a (in kcal/mol) for the hindered rotation of the amide groups of **1**, **2** and **3** around the CN bond, estimated by the line shape analysis of ^1H and ^{13}C NMR spectra.

Compound	Solvent	Observed nucleus	Observed group	E_a
1	$(\text{CD}_3)_2\text{CO}$	^{13}C	OCH_2	15.4 ± 0.6
	CDCl_3	^{13}C	OCH_2	13.5 ± 0.5
		^{13}C	NCH_2	12.9 ± 0.4
		^1H	CH_2	16 ± 1
	CD_3OD	^1H	CH_2	17.1 ± 0.2
2	$(\text{CD}_3)_2\text{CO}$	^1H	NCH_2	17.0 ± 0.3
	$\text{THF-}d_8$	^1H	NCH_2	15.8 ± 0.5
3	$(\text{CD}_3)_2\text{CO}$	^1H	CH_3	13.9 ± 0.7
	CDCl_3	^1H	CH_3	15.3 ± 0.5

insufficient to address this multi-parametric problem in full, in Fig. 4 we plot the experimentally estimated barrier heights as a function of OH chemical shift, which can be considered as a measure for the hydrogen bond strength (shortness) [43]. For this plot we have selected the OH chemical shifts measured at lowest temperature for each solvent, so that the values are less influenced by any possible residual fast equilibria, associated with opening/closing of intramolecular OHO bond. The complete dataset of temperature dependent OH chemical shift can be found in Tables S2–S4 of Supplementary data. From Fig. 4 it follows that the energy barrier has a tendency to increase together with the hydrogen bond strength (electronic effect). Though the dependence of the rotational barrier height on the strength of the hydrogen bond has been previously observed in some cases, Refs. [14–18], caution should be used in interpretation of the plot in Fig. 4, as steric hindrances and solvent interactions could also be quite substantial. Fig. 4 shows noticeable data point scattering and works better as a general trend rather than a predictive tool for each individual compound. Further discussion of the rotational barriers will be given below based on DFT calculations.

An interesting spectral feature can be seen at lowest temperatures in ^1H NMR spectra presented in Fig. 1. When the temperature is lowered below 250 K all four signals of CH_2 groups of morpholine ring become somewhat broader, but the one at the lowest field broadens to such an extent that at 220 K it becomes almost invisible. A rationalization of this phenomenon can be achieved taking

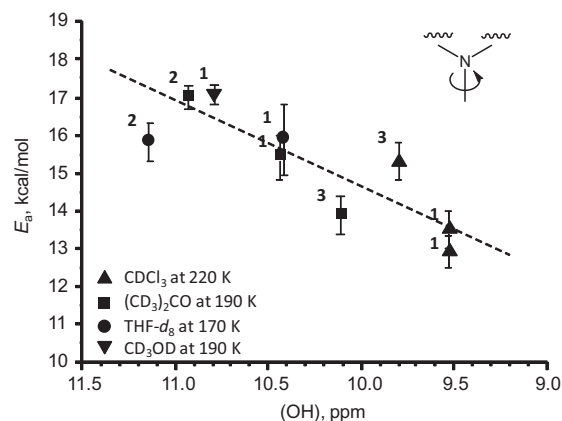


Fig. 4. Activation energies E_a for the rotation around amide CN bonds in **1**, **2** and **3** dissolved in various solvents, obtained by line shape analysis of NMR data, versus experimental values of OH chemical shifts.

into account further dynamics which is possible in the molecule. Firstly, the morpholine ring is not planar and it can undergo conformational isomerism (sort of chair–chair ‘ring-flip’), shown as ‘a’ in Scheme 3, where the molecule is oriented in such a way that the naphthalene ring – shown as a gray bar – is perpendicular to the plane of the paper (the amide fragment is planar, but this plane does not coincide with the naphthalene plane). Adding this chair–chair ‘ring flip’ to the rotation around the CN bond we arrive to the dynamics scheme shown as ‘b’ in Scheme 3 (as in this scheme we focus on the morpholine moiety, the rest of the molecule is depicted simply as R).

Secondly, the amide group can pass through the naphthalene plane as a result of an incomplete rotation around the CC bond, in fact a twisting around the CC bond by $60\text{--}70^\circ$ without breaking the OHO hydrogen bond. Adding this to Scheme 3 we get the overall dynamics as shown in Scheme 4, where one of the CH_2 groups is marked with an asterisk to make it easier to follow the CN rotation.

When the ‘ring flip’ and ‘CC twisting’ dynamic processes slow down in NMR time scale, the signals of CH_2 protons should split and the chemical shift difference is likely to be the largest for those protons which are closest to the naphthalene rings and affected by its ring currents. In our experiments temperature was sufficiently low to broaden the signals but not low enough to actually see the splitting.

Morpholine ring dynamics can be further corroborated by DFT calculations. Fully optimized (B3LYP/6-31+G(d,p)) structures of **1**, **2** and **3** are shown in Fig. 5. Atom labeling is added to key atoms which will be used in discussion below. In global minimum all three molecules exhibit intramolecular OHO hydrogen bonds. As mentioned above, the amide group, which is planar by itself, is located out of the plane of naphthalene rings and so is the OHO hydrogen bond.

Besides, both conformational isomers shown in Scheme 3a can be optimized as local energy minima on the conformational landscape; additional minimum corresponds to the intermediate structure with partially inverted morpholine ring (see structures A, C and B in Fig. 6).

Conformers A and C are very close in energy and both are not too far from conformer B if the OHO hydrogen bond is intact (top row in Fig. 6). The energy separation between all three conformers increases noticeably if OHO is broken (bottom row in Fig. 6).

Potential energy profiles for the rotation of the amide group around C11-N1 (CN) or C2-C11 (CC) bonds of **1**, **2** and **3** are plotted as ‘a’ and ‘b’ in Fig. 7, respectively. As rotational coordinates we have chosen C2-C11-N1-C12 and C1-C2-C11-N1 dihedral angles. Some roughness of the given datasets is due to the fact that during

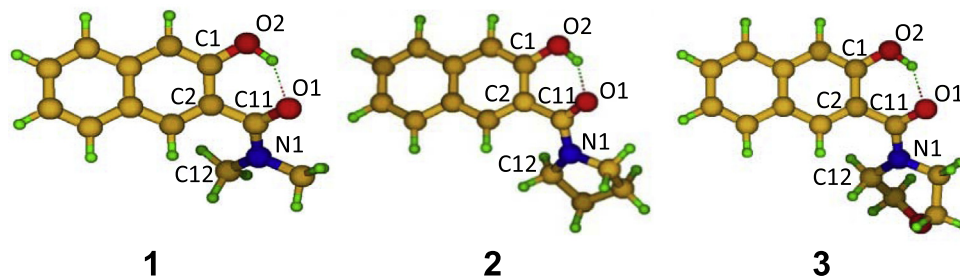


Fig. 5. Optimized structures (B3LYP/6-31+G(d,p)) of **1**, **2** and **3**.

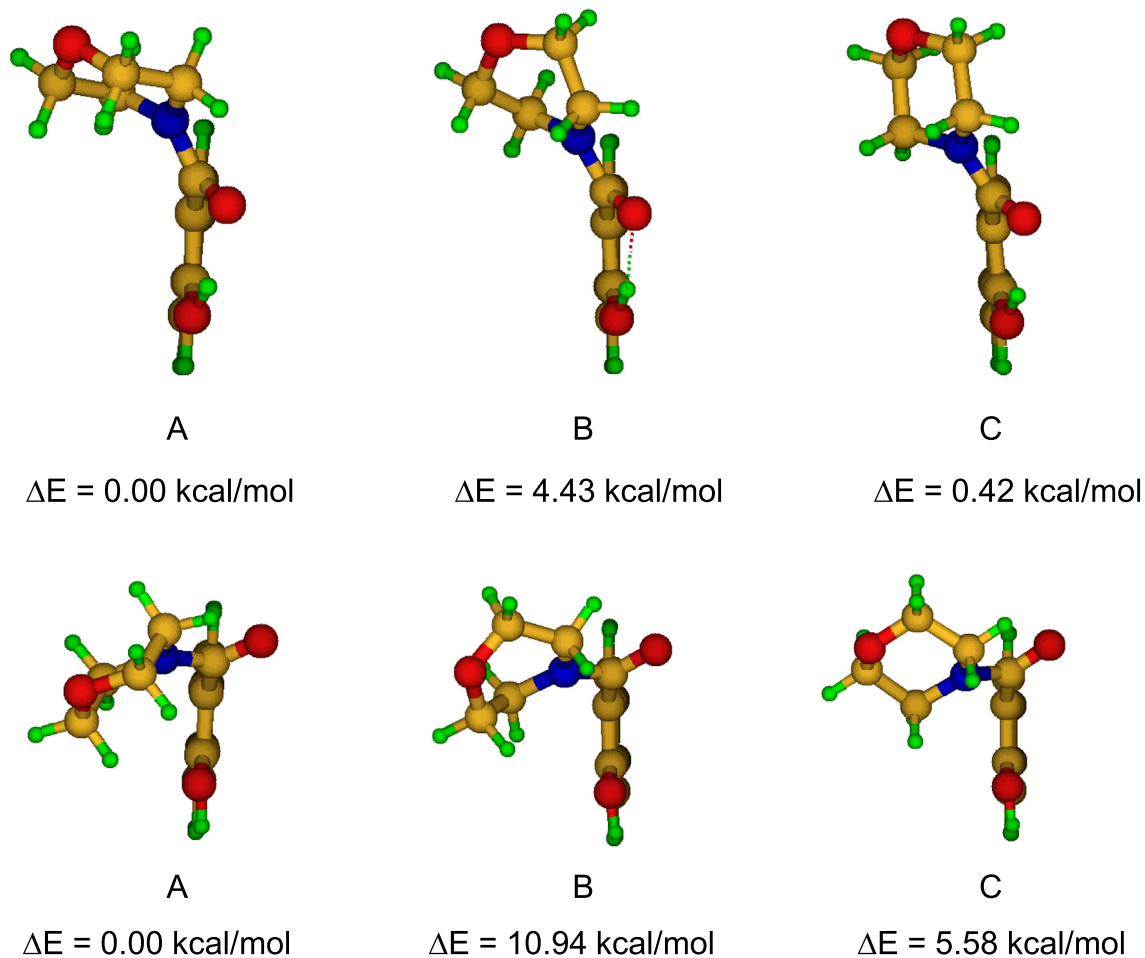


Fig. 6. Calculated (B3LYP/6-31+G(d,p)) optimized structures of the conformational isomers of **1**, corresponding to three steps of the morpholine ring inversion.

do not take solvent into account, we do not expect to see the numerical coincidence with the experiment, but roughly the calculated E_a values are similar to the experimental ones. Unfortunately, there is no apparent correlation between the energy barriers and the hydrogen bond strength (shortness), represented either as the $r(\text{O} \cdots \text{O})$ or as the sum $r(\text{O} \cdots \text{H}) + r(\text{H} \cdots \text{O})$ [43].

Rotation around the CC bond leads to a potential energy curve with several minima and maxima ('b' in Fig. 7). These extrema have clear physical meaning. Two minima at ca. 140° and 210° correspond to the structures with OHO hydrogen bonds. These minima are separated by a 70° turn around the CC bond without breaking the OHO bond and a barrier of 3–4 kcal/mol, which reflects the steric repulsion when the amide group comes into the plane of naphthalene rings (the process which was called 'CC twist' above). Second pair of energy minima (ca. 40° and

320°) corresponds to structures with rather unstable OHN bonds. These are 5–8 kcal/mol higher than the global minimum. Interestingly, the calculated barrier height for the complete 360° rotation around the CC bond is comparable with the CN rotation barrier, so that under experimental conditions at room temperature one could expect to observe both rotations happening at comparable rates. However, fast 360° turns do not affect NMR spectra and we cannot confirm or disconfirm this computational finding.

In summary, the hypothesis of the morpholine ring dynamics is fairly justified by computational results. Comparing experimental and computed value of the CN rotation activation barrier and computed energy barriers for chair–chair 'ring flip' or a 'CC twist' we can indeed conclude that upon cooling first the CN rotation should slow down and then the 'chair flip'/CC twist'.

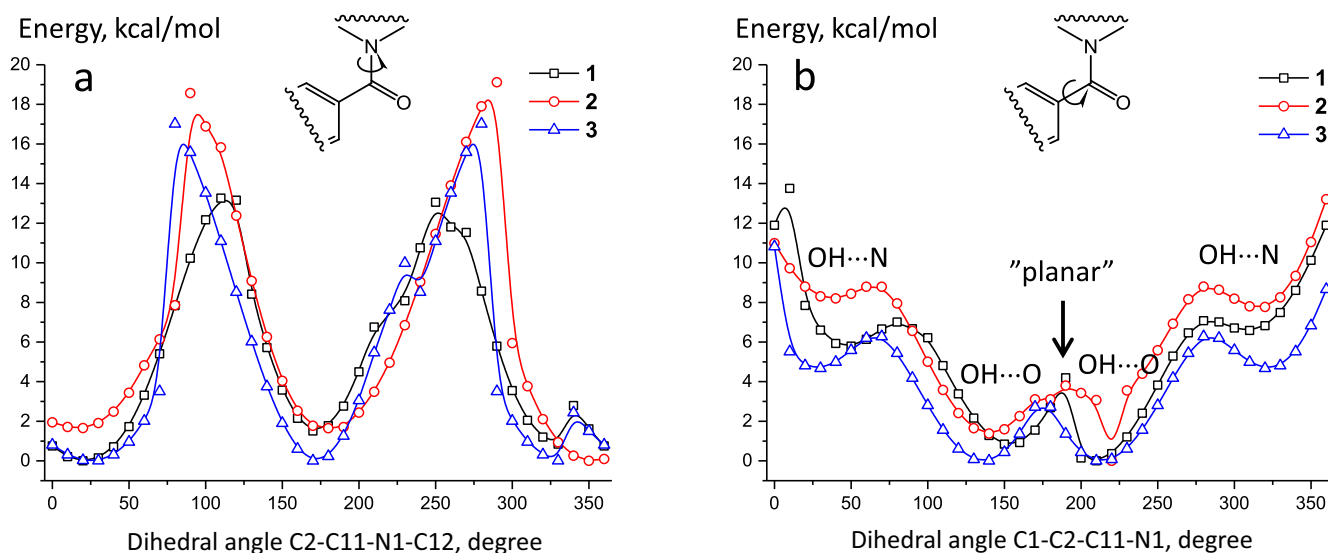


Fig. 7. Calculated (B3LYP/6-31+G(d,p)) potential energy curves for the rotation of amide group around (a) CN and (b) CC bond in **1**, **2** and **3**. For atom labeling see Fig. 5. Data points are connected by smooth curves.

Table 3

Energy barriers E_a (in kcal/mol) for the hindered rotation of the amide groups of **1**, **2** and **3** around the CN bond, calculated at B3LYP/6-31+G(d,p) level of theory as well as interatomic distances in the intramolecular OHO hydrogen bonds (in Å).

Compound	E_a	$r(\text{O}\cdots\text{H})$	$r(\text{H}\cdots\text{O})$	$r(\text{O}\cdots\text{O})$	$r(\text{O}\cdots\text{H}) + r(\text{H}\cdots\text{O})$
1	13.2 ± 0.2	0.987	1.737	2.614	2.724
2	18.9 ± 0.4	0.988	1.719	2.600	2.707
3	17.0 ± 0.2	0.981	1.770	2.635	2.751

Conclusions

Conformational dynamics and hydrogen bonding – anticipated phenomena for all compounds involving amide groups – have been studied here for a new set of compounds, beta-hydroxynaphthylamides. On the basis of variable-temperature ^1H and ^{13}C NMR spectra and DFT calculations we conclude that in polar aprotic medium (solution-state, experiment) and in vacuum (gas-phase, calculations) the energetically preferred conformers of β -hydroxynaphthylamides **1**, **2** and **3** are the non-planar structures with intramolecular $\text{OH}\cdots\text{O}$ hydrogen bonds. In contrast, in the solid state **1** and **3** form intermolecularly $\text{OH}\cdots\text{O}$ hydrogen bonded chains. Energy barriers for the amide group rotation around the CN bond were experimentally estimated; the barrier heights lie in the region 13–19 kcal/mol and appear to correlate with the hydrogen bond strength, measured as OH proton NMR chemical shift. Such interdependence can be explained as the result of the partial electron transfer to the carbonyl oxygen atoms, which increases the double bond character of the CN bond and thus increases the rotational barrier. Finally, additional dynamic process in **1** was detected, which is likely to be morpholine ring inversion (chair-chair ‘ring flip’, not the inversion of nitrogen) and ‘twisting’ around the CC bond without breaking the OHO hydrogen bond (not a complete CC rotation) as shown in Scheme 4.

Acknowledgements

The authors acknowledge the Wrocław Center for Networking and Supercomputing (WCSS) for generous grants of computer time, Center for Magnetic Resonance (St. Petersburg) for the NMR

measurements, St. Petersburg State University (Russia) and Wrocław University (Poland) for travel grants, RFBR Grant 14-03-00111 (P.T.; NMR studies, DNMR analysis) and the grant of the Polish Plenipotentiary in JINR Nr 118 from 05.02.2014, p.7 for partial financial support.

Appendix A. Supplementary data

Supplementary data associated with this article can be found, in the online version, at <http://dx.doi.org/10.1016/j.saa.2015.04.052>.

References

- [1] E.G. Buchanan, W.H. James III, S.H. Choi, L. Guo, S.H. Gellman, C.W. Müller, T.S. Zwier, *J. Chem. Phys.* 137 (2012) 094301–094316.
- [2] H. Torii, *J. Phys. Chem. Lett.* 3 (2012) 112–116.
- [3] A. Genshaft, J.-A.S. Moser, E.L. D’Antonio, C.M. Bowman, D.W. Christianson, *Proteins* 81 (2013) 1051–1057.
- [4] A. Buczek, R. Wałęsa, M.A. Broda, *Biopolymers* 97 (2012) 518–528.
- [5] N.Yu. Gorobets, S.A. Yermolayev, T. Gurley, A.A. Gurinov, P.M. Tolstoy, I.G. Shenderovich, N.E. Leadbeater, *J. Phys. Org. Chem.* 25 (2012) 287–295.
- [6] E. Kleinpeter, *J. Mol. Struct.* 380 (1996) 139–156.
- [7] A.R. Modaresi-Alam, P. Najafi, M. Rostamizadeh, H. Keykha, H.-R. Bijanzadeh, E. Kleinpeter, *J. Org. Chem.* 72 (2007) 2208–2211.
- [8] J. Chen, P.G. Willis, S. Parkin, A. Cammers, *Eur. J. Org. Chem.* (2005) 171–178.
- [9] E.A. Skorupska, R.B. Nazarski, M. Ciechanska, A. Jozwiak, A. Klys, *Tetrahedron* 69 (2013) 8147–8154.
- [10] T. Dürst, A. Gryff-Keller, J. Terpinski, *Org. Magn. Reson.* 21 (1983) 657–661.
- [11] R. Wanke, L. Benisvy, M.L. Kuznetsov, M.F.C. Guedes da Silva, A.J.L. Pombeiro, *Chem. Eur. J.* 17 (2011) 11882–11892.
- [12] M.C. Etter, Z. Urbanczyk-Lipkowska, T.M. Ameli, T.W. Panunto, *J. Crystallogr. Spectrosc. Res.* 18 (1988) 491–508.
- [13] V. Arjunan, M. Kalaivani, P. Ravindran, S. Mohan, *Spectrochim. Acta A* 79 (2011) 1886–1895.
- [14] E. Velcheva, B. Stamboliyska, *J. Mol. Struct.* 875 (2008) 264–271.
- [15] P. Majewska, J. Pająk, M. Rospenk, A. Filarowski, *J. Phys. Org. Chem.* 22 (2008) 130–137.
- [16] L. Guo, Q.-L. Wang, Q.-Q. Jiag, Q.-J. Jiang, Y.-B. Jiang, *J. Org. Chem.* 72 (2007) 9947–9953.
- [17] P. Kowski, A. Kochel, M.G. Perevozskina, A. Filarowski, *J. Mol. Struct.* 790 (2006) 65–73.
- [18] W.B. Jennings, D. Randall, B.M. Saket, *J. Chem. Soc. Chem. Commun.* (1982) 508–509.
- [19] G. Bartoli, S. Grilli, L. Lunazzi, M. Massaccesi, A. Mazzanti, S. Rinaldi, *J. Org. Chem.* 67 (2002) 2659–2664.
- [20] H. Suezawa, K. Tsuchiva, E. Tahara, H. Minoru, *Bull. Chem. Soc. Jpn.* 60 (1987) 3973–3978.
- [21] A. Filarowski, A. Koll, L. Sobczyk, *Curr. Org. Chem.* 13 (2009) 172–193.

- [22] A. Filarowski, A. Koll, P.E. Hansen, M. Kluba, *J. Phys. Chem. A* 112 (2008) 3478–3485.
- [23] M. Rospenk, L. Sobczyk, P. Schah-Mohammed, H.-H. Limbach, N.S. Golubev, S.M. Melikova, *Magn. Res. Chem.* 39 (2001) S81–S90.
- [24] G.S. Denisov, V.A. Gindin, N.S. Golubev, A.I. Koltsov, S.N. Smirnov, M. Rospenk, A. Koll, L. Sobczyk, *Magn. Res. Chem.* 31 (1993) 1034–1037.
- [25] S.T. Ali, L. Antonov, W.M.F. Fabian, *J. Phys. Chem. A* 118 (2014) 778–789.
- [26] W.M.F. Fabian, L. Antonov, D. Nedeltcheva, F.S. Kamounah, P.J. Taylor, *J. Phys. Chem. A* 108 (2004) 7603–7612.
- [27] L. Antonov, W.M.F. Fabian, P.J. Taylor, *J. Phys. Org. Chem.* 18 (2005) 1169–1175.
- [28] M. Chan-Huot, S. Sharif, P.M. Tolstoy, M.D. Toney, H.-H. Limbach, *Biochemistry* 49 (2010) 10818–10830.
- [29] M.J. Frisch, G.W. Trucks, H.B. Schlegel, G.E. Scuseria, M.A. Robb, J.R. Cheeseman, G. Scalmani, V. Barone, B. Mennucci, G.A. Petersson, H. Nakatsuji, M. Caricato, X. Li, H.P. Hratchian, A.F. Izmaylov, J. Bloino, G. Zheng, J.L. Sonnenberg, M. Hada, M. Ehara, K. Toyota, R. Fukuda, J. Hasegawa, M. Ishida, T. Nakajima, Y. Honda, O. Kitao, H. Nakai, T. Vreven, J.A. Montgomery Jr., J.E. Peralta, F. Ogliaro, M. Bearpark, J.J. Heyd, E. Brothers, K.N. Kudin, V.N. Staroverov, R. Kobayashi, J. Normand, K. Raghavachari, A. Rendell, J.C. Burant, S.S. Iyengar, J. Tomasi, M. Cossi, N. Rega, N.J. Millam, M. Klene, J.E. Knox, J.B. Cross, V. Bakken, C. Adamo, J. Jaramillo, R. Gomperts, R.E. Stratmann, O. Yazyev, A.J. Austin, R. Cammi, C. Pomelli, J.W. Ochterski, R.L. Martin, K. Morokuma, V.G. Zakrzewski, G.A. Voth, P. Salvador, J.J. Dannenberg, S. Dapprich, A.D. Daniels, Ö. Farkas, J.B. Foresman, J.V. Ortiz, J. Cioslowski, D.J. Fox, Gaussian 09, Revision D01, Gaussian Inc., Wallingford CT, 2009.
- [30] A.D. Becke, *J. Chem. Phys.* 98 (1993) 5648–5652.
- [31] C. Lee, W. Yang, R.G. Parr, *Phys. Rev.* 37 (1993) B785–B789.
- [32] (a) A.D. McLean, G.S. Chandler, *J. Chem. Phys.* 72 (1980) 5639–5648;
(b) R. Krishnan, J.S. Binkley, R. Seeger, J.A. Pople, *J. Chem. Phys.* 72 (1980) 650–654;
(c) T. Clark, J. Chandrasekhar, G.W. Spitznagel, P. von Rauge Schleyer, *J. Comput. Chem.* 4 (1983) 294–301;
(d) M.J. Frisch, J.A. Pople, J.S. Binkley, *J. Chem. Phys.* 80 (1984) 3265–3269.
- [33] S. Scheiner, *Hydrogen Bonding: A Theoretical Perspective*, Oxford University Press, New York, 1997.
- [34] CrysAlisPro, Agilent Technologies, Version 1.171.35.19.
- [35] G.M. Sheldrick, SHELXS97 Program for Solution of Crystal Structure, University of Goettingen, Germany, 1997.
- [36] G.M. Sheldrick, SHELXL97 Program for Refinement of Crystal Structure, University of Goettingen, Germany, 1997.
- [37] E. Kleinpeter, in: E. Juaristi (Ed.), *Conformational Behavior of Six-Membered Rings. Analysis, Dynamics and Stereoelectronic Effects*, VCH Publishers, New York, Weinheim, Cambridge, 1995, pp. 201–243 (Chapter 6).
- [38] E. Kleinpeter, in: A. Katritzky (Ed.), *Advances in Heterocyclic Chemistry*, 69, Elsevier, Amsterdam, 1996, pp. 41–126 (Chapter 2).
- [39] E. Kleinpeter, in: A. Katritzky (Ed.), *Advances in Heterocyclic Chemistry*, 69, Elsevier, Amsterdam, 1996, pp. 217–269 (Chapter 4).
- [40] A. Mazzanti, D. Casarini, *WIREs Comput. Mol. Sci.* 2 (4) (2012) 613–641.
- [41] B. Koeppel, P.M. Tolstoy, H.-H. Limbach, *J. Am. Chem. Soc.* 133 (2011) 7897–7908.
- [42] M. Sigalov, B. Shainyan, N. Chipanina, I. Ushakov, A. Shulunova, *J. Phys. Org. Chem.* 22 (2009) 1178–1187.
- [43] P.M. Tolstoy, J. Guo, B. Koeppel, N.S. Golubev, G.S. Denisov, S.N. Smirnov, H.-H. Limbach, *J. Phys. Chem. A* 114 (2010) 10775–10782.
- [44] J. Guo, P.M. Tolstoy, B. Koeppel, G.S. Denisov, H.-H. Limbach, *J. Phys. Chem. A* 115 (2011) 9828–9836.
- [45] M.V. Sigalov, B.A. Shainyan, N.N. Chipanina, L.P. Oznobikhina, *J. Phys. Chem. A* 117 (2013) 11346–11356.
- [46] H.-H. Limbach, P.M. Tolstoy, N. Perez-Hernandez, J. Guo, I.G. Shenderovich, G.S. Denisov, *Isr. J. Chem.* 49 (2009) 199–216.
- [47] P.M. Tolstoy, S.N. Smirnov, I.G. Shenderovich, N.S. Golubev, G.S. Denisov, H.-H. Limbach, *J. Mol. Struct.* 700 (2004) 19–27.
- [48] I.G. Shenderovich, A.P. Burtsev, G.S. Denisov, N.S. Golubev, H.-H. Limbach, *Magn. Reson. Chem.* 39 (2001) S91–S99.
- [49] C.F. Macrae, I.J. Bruno, J.A. Chisholm, P.R. Edgington, P. McCabe, E. Pidcock, L. Rodriguez-Monge, R. Taylor, J. van de Streek, P.A. Wood, *J. Appl. Crystallogr.* 41 (2008) 466–470.